Apoptosis (2013) 18:1536–1547
DOI 10.1007/s10495-013-0885-8

ORIGINAL PAPER

Inhibition of polyamine oxidase prevented cyclin-dependent kinase inhibitor-induced apoptosis in HCT 116 colon carcinoma cells

Ajda Çoker Gürkan · Elif Damla Arısan · Pınar Obakan · Narçin Palavan-Ünsal

Published online: 28 July 2013

Abstract Roscovitine and purvalanol are novel cyclin-dependent kinase (CDK) inhibitors that prevent cell proliferation and induce apoptotic cell death in various cancer cell lines. Although a number of studies have demonstrated the potential apoptotic role of roscovitine, there is limited data about the therapeutic efficiency of purvalanol on cancer cells. The natural polyamines (PAs) putrescine, spermidine, and spermine have essential roles in the regulation of cell differentiation, growth, and proliferation, and increased levels of these compounds have been associated with cancer progression. Recently, depletion of intracellular PA levels because of modulation of PA catabolic enzymes was shown to be an indicator of the efficacy of chemotherapeutic agents. In this study, our aim was to investigate the potential role of PA catabolic enzymes in CDK inhibitor-induced apoptosis in HCT 116 colon carcinoma cells. Exposure of cells to roscovitine or purvalanol decreased cell viability in a dose- and time-dependent manner. The selected concentrations of roscovitine and purvalanol inhibited cell viability by 50 % compared with control cells and induced apoptosis by activating the mitochondria-mediated pathway in a caspase-dependent manner. However, the apoptotic effect of purvalanol was stronger than that of roscovitine in HCT 116 cells. In addition, we found that CDK inhibitors decreased PA levels and significantly upregulated expression of key PA catabolic enzymes such as polyamine oxidase (PAO) and spermine oxidase (SMO). MDL-72,527, a specific inhibitor of PAO and SMO, decreased apoptotic potential of CDK inhibitors on HCT 116 cells. Moreover, transient silencing of PAO was also reduced prevented CDK inhibitor-induced apoptosis in HCT 116 cells. We conclude that the PA catabolic pathway, especially PAO, is a critical target for understanding the molecular mechanism of CDK inhibitor-induced apoptosis.

Keywords Colon cancer · Apoptosis · CDK Inhibitors · Polyamine catabolism

A. Ç. Gürkan · E. D. Arısan (✉) · P. Obakan · N. Palavan-Ünsal
Molecular Biology and Genetics Department, Science and Literature Faculty, Istanbul Kultur University, Atakoy Campus, 34156 Istanbul, Turkey
e-mail: d.arisan@iku.edu.tr

Introduction

Cyclin-dependent kinases (CDKs) regulate the eukaryotic cell cycle by binding specific cyclin targets and catalyzing protein phosphorylation, which is essential in DNA synthesis [1]. CDK-cyclin complex formation is involved in cell growth, proliferation, and differentiation processes [2]. Therefore, complex formation during the cell cycle is a critical target in therapeutic strategies aimed at preventing cell proliferation and inducing apoptosis in cancer cells [3]. The novel CDK inhibitors roscovitine (CYC202 or seliciclib) and purvalanol are strong inducers of apoptosis that prevent binding of CDKs to their cyclin targets and cause cell cycle arrest [4, 5]. Recent studies showed that roscovitine and purvalanol induced apoptosis by causing cell cycle arrest at the G1 and G2/M phases in prostate [6], breast [7], lung [8], multiple myeloma [9], and colon cancer [10] cell lines.

The natural polyamines (PAs) putrescine, spermidine, and spermine are polycationic amine derivatives [11, 12] that act as essential molecules in cellular processes such as cell cycle regulation, cell proliferation and differentiation, and tumor growth [13–15]. The role of PAs in the

regulation of cell survival and apoptotic cell death is still unclear. Because of their cationic properties, PAs are implicated as protective substances against apoptosis, and intracellular PA content was found to be elevated in malignant cells [12]. Consistent with this finding, ornithine decarboxylase (ODC), an enzyme of the PA biosynthetic pathway, was found to be overexpressed in tumor tissues [16, 17]. An activated PA catabolic pathway induces the accumulation of toxic substances through the conversion of PAs to oxidized derivatives, which might enhance the potential of therapeutic drugs [18, 19]. The intracellular PA pool is under the control of PA catabolic enzymes: spermidine/spermine N^1-acetyltransferase (SSAT), spermine oxidase (SMO), and N^1-acetylpolyamine oxidase (PAO) [19, 20]. Recent findings indicate that chemotherapeutic drugs such as 5-fluorouracil or oxaliplatin might upregulate expression of the SSAT gene in colorectal cancer cells while inducing apoptosis [21]. Similarly, we previously found that silencing of the SSAT gene might prevent CDK inhibitor-induced apoptosis in CaCo-2 colon carcinoma cells [22]. In addition, PA depletion is critical for the apoptotic decision in HCT 116 colon carcinoma cells treated with roscovitine [23]. A better understanding of the molecular basis of the PA metabolic pathway, which plays a critical role in programmed cell death, might lead to new strategies for cancer therapy.

In the present study, we demonstrate that roscovitine or purvalanol treatment causes a significant increase in apoptotic cell populations by inducing cell cycle arrest and activating the mitochondrial pathway in HCT 116 colon carcinoma cells. Both CDK inhibitors decreased the intracellular PA content by upregulating the expression of SMO and PAO. Cells exposed to roscovitine or purvalanol in the presence of MDL-72,527 (a specific inhibitor of SMO and PAO, *N*,*N*′-bis(2,3-butadienyl)-1,4-butanediamine dihydrochloride) or with transient silencing of the PAO gene (using PAO siRNA) had lower levels of poly (ADP-ribose) polymerase (PARP) cleavage than cells exposed to the drug alone.

Materials and methods

Drugs, chemicals, and antibodies

Roscovitine was purchased from Sigma (St. Louis, MO, USA), dissolved in DMSO to make a 10 mM stock solution, and stored at −20 °C. Purvalanol was purchased from Tocris Bioscience (Bristol, UK) and dissolved in DMSO at an initial stock concentration of 10 mM. Z-VAD-FMK (general caspase inhibitor) was purchased from BD Biosciences (San Jose, CA, USA). MDL-72,527 (PAO/SMO inhibitor) and putrescine, spermidine, and spermine standards (each 10 mM) were purchased from Sigma. *N*-acetylcysteine and 2′,7′-dichlorofluorescein (DCFH-DA) were purchased from Calbiochem (San Diego, CA, USA).

Rabbit antibodies to CDK1 (1:1,000), CDK2 (1:1,000), CDK4 (1:1,000), CDK7 (1:1,000), CDK9 (1:1,000), cyclin A (1:1,000), cyclin B1 (1:2,000), cyclin D3 (1:2,000), cyclin E (1:2,000), β-actin (1:2,000), p53 (1:1,000), p21 (1:1,000), retinoblastoma tumor suppressor protein (Rb) (1:1,000), phospho-Rb (Ser795) (1:1,000), phospho-Rb (Ser807/Ser811) (1:1,000), pro-caspase-3 (1:1,000), pro-caspase-9 (1:1,000), cleaved caspase-7 (1:1,000), cleaved caspase-9 (1:1,000), Puma (1:1,000), Noxa (1:1,000), and COX IV (1:1,000) were purchased from Cell Signaling Technology (Danvers, MA, USA). Mouse antibodies to Bad (1:1,000), Bax (1:1,000), Bcl-2 (1:1,000), and PARP (1:1,000) were purchased from BD Biosciences. Rabbit antibodies to ODC, SSAT, and PAO (1:1,000) and PAO siRNA were purchased from Santa Cruz Biotechnology (Santa Cruz, CA, USA). Mouse antibody to cytochrome *c* (1:1,000) was purchased from Biovision (Milpitas, CA, USA). Rabbit antibody to SMO (1:1,000) was a gift from Dr. Robert Casero (Johns Hopkins University, Baltimore, MD, USA). Rabbit antibodies to ODC antizyme 1 (OAZ1) and antizyme inhibitor 1 (AZI) were purchased from Abcam (Cambridge, UK). Horseradish peroxidase-conjugated secondary anti-rabbit and anti-mouse antibodies (1:5,000) were from Cell Signaling Technology.

Cell culture

HCT 116 (CCL-247) colon carcinoma cells were purchased from ATCC (Manassas, VA, USA). Cells were maintained in McCoy's medium (PAN Biotech, Aidenbach, Germany) with 2 mM L-glutamine, 10 % fetal calf serum (PAN Biotech), 1 % non-essential amino acids (Biological Industries, Kibbutz Beit Haemek, Israel), 100 U/ml penicillin, and 100 μg/ml streptomycin (Biological Industries) and grown in the presence of 5 % CO_2 in humidified air at 37 °C.

Cell viability assay

The effect of CDK inhibitors on cell viability was determined by a colorimetric MTT (3-(4,5-dimethylthiazol-2-yl)-2,5-diphenyltetrazolium bromide) assay (Roche, Indianapolis, IN, USA). HCT 116 cells were plated at a density of 1×10^5 cells/well in 96-well plates, allowed to attach overnight, and treated for 24 h with various concentrations (0–75 μM) of roscovitine or purvalanol. After the 24 h treatment, 20 μl of MTT (5 mg/ml) was added to the culture medium for 4 h. Following aspiration of medium, 200 μl of DMSO was added to dissolve the formazan crystals. The absorbance of the suspension at 570 nm was

measured with a microplate reader (Bio-Rad, Hercules, CA, USA).

Cell proliferation assay

HCT 116 cells were seeded on 6-well plates (1×10^6 cells/well) and treated with roscovitine (50 μM) or purvalanol (30 μM) for 72 h. Every 24 h, cells were trypsinized and stained with trypan blue, and viable and dead cells were counted under a light microscope. Cell proliferation ratio in control and CDK inhibitor-treated samples were evaluated by plotting the number of cells against the time since initiation of treatment.

Apoptosis detection by ELISA

Amounts of cytoplasmic histone-associated DNA fragments (mono- and oligonucleosomes) were determined according to the instructions provided with the Cell Death Detection ELISA^{PLUS} assay (Roche, Indianapolis, IN, USA). HCT 116 cells were seeded in 96-well plates at a density of 1×10^5 cells/well, allowed to attach, and treated with roscovitine (50 μM) or purvalanol (30 μM) for 24 h. Cell lysates were placed in a streptavidin-coated microplate. A mixture of anti-histone–biotin and anti-DNA–peroxidase was added and incubated for 2 h at 15–25 °C. After removal of unbound antibodies by a washing procedure, the amount of peroxidase was determined photometrically at 405 nm with ABTS as a substrate.

DNA fragmentation analysis

Exponentially growing HCT 116 cells were seeded at a density of 3×10^5 cells/well in 6-well plates in drug-free medium. They were incubated overnight to allow attachment to the plates and then treated with roscovitine (50 μM) or purvalanol (30 μM) for 24 h. Cell lysates were extracted with lysis buffer (10 mM Tris (pH 8.0), 20 mM EDTA) for 1 h on ice. DNA fragments were separated by phenol/chloroform extraction and centrifugation for 15 min at 13,200 rpm. DNA was precipitated from supernatants with 3 M sodium acetate and isopropanol at −20 °C overnight. Pellets were recovered by centrifugation at 13,200 rpm for 10 min, air-dried, and then resuspended in 20 μl of TE buffer. Following electrophoresis on 2 % agarose gel for 2 h, isolated DNA fragments were visualized using a UV transilluminator.

Cell cycle analysis by propidium iodide staining

HCT 116 cells were seeded in 6-well plates at a density of 2×10^5 cells/well and then treated with roscovitine (50 μM) or purvalanol (30 μM) for 24 h. Both floating and adherent cells were collected and fixed with 70 % ethanol. Following incubation on ice for 30 min, samples were diluted with 1× PBS and then centrifuged at 1,200 rpm for 5 min. Pellets were resuspended in 1× PBS with RNase (100 μg/ml) and propidium iodide (40 μg/ml). Samples were kept at 37 °C for 30 min in the dark. The cell cycle distribution was analyzed using a FACScan flow cytometer (Becton–Dickinson, Oxford, England).

Detection of mitochondrial membrane potential (MMP)

HCT 116 cells were seeded on 12-well plates (1×10^5 cells/well). Following a 2 h pretreatment with general caspase inhibitor (10 μM Z-VAD-FMK), HCT 116 cells were treated with CDK inhibitors for 24 h. The cells were washed once with 1× PBS and then stained with a fluorescent probe, 3,3′-dihexyloxacarbocyanine iodide ($DiOC_6$) (4 nM). MMP was visualized under a fluorescence microscope (Olympus, Japan) and measured with a Fluoroskan Ascent fluorometer (Thermo Labsystems, Beverly, MA, USA) (excitation/emission = 488/538 nm).

Immunoblot analysis

HCT 116 cells were treated with the appropriate concentrations of each CDK inhibitor for 24 h. Cells were then washed with ice-cold 1× PBS and lysed on ice in a solution containing 20 mM Tris–HCl (pH 7.5), 150 mM NaCl, 0.5 % Nonidet P-40 (v/v), 1 mM EDTA, 0.5 mM PMSF, 1 mM DTT, and protease inhibitor cocktail (Complete, Roche, Indianapolis, IN, USA). After cell lysis, cell debris was removed by centrifugation for 15 min at 13,200 rpm, and protein concentrations were determined by Bradford assay. Total protein lysates (30 μg) were separated by 12 % SDS-PAGE and transferred onto PVDF membranes (Roche). The membranes were then blocked with 5 % milk blocking solution in Tris-buffered saline (TBS) with Tween 20 (Sigma, St. Louis, MO, USA) and incubated with appropriate primary antibodies and horseradish peroxidase-conjugated secondary antibodies in antibody buffer containing 5 % (v/v) milk blocking solution. Following a washing step with 1× TBS–Tween 20, proteins were analyzed using an enhanced chemiluminescence detection system [24] and Lumi-Film Chemiluminescent Detection Film (Complete, Roche). Immunoblotting experiments were repeated at least twice and the ImageJ software (Bethesda, MD, USA) was used to measure band intensities. Band intensities are shown below the western blot images.

Polyamine determination

Cellular PA content was determined by HPLC analysis following a benzoylation procedure. HCT 116 cells

(1.2×10^6) were seeded in 100 mm Petri dishes and allowed to attach overnight. The cells were then treated with the desired concentration of roscovitine or purvalanol for 24 h. Following washing of cells with 1× PBS, cell lysates were obtained by scraping. The scraped cell lysates were transferred to a new microfuge tube and 50 % trichloroacetic acid was added to each sample (1:10, v/v). All samples were kept at −20 °C until the benzoylation process. Following benzoylation, samples were immediately run on the HPLC system (Agilent, Santa Clara, CA, USA) using a UV detector set at 226 mV. Results were evaluated against the internal standard 1,7-diaminoheptane and the standard curve of putrescine, spermidine, and spermine standards.

Determination of reactive oxygen species (ROS) by DCFH-DA staining

HCT 116 cells were seeded in 96-well plates (1×10^4 cells/well). Following exposure of cells to roscovitine or purvalanol for 24 h, media was carefully discarded and cells were stained with DCFH-DA (0.5 μM). Drug-induced ROS generation in treated samples and untreated control samples was visualized using fluorescence microscopy (200×).

Transient silencing of PAO

HCT 116 cells were placed in a 6-well plate. Cells were transfected with PAO siRNA (1.25 μg) using a 1:3 ratio of siRNA and RNAiFect transfection reagent (Qiagen GmbH, Hilden, Germany), following the manufacturer's protocol. CDK inhibitors were added 48 h after transfection, and cells were incubated for 24 h.

Statistical analysis

All samples were evaluated statistically using an Excel calculation file. The MTT assay and cell death ELISA results are shown as mean ± SD, and Student's *t* test was

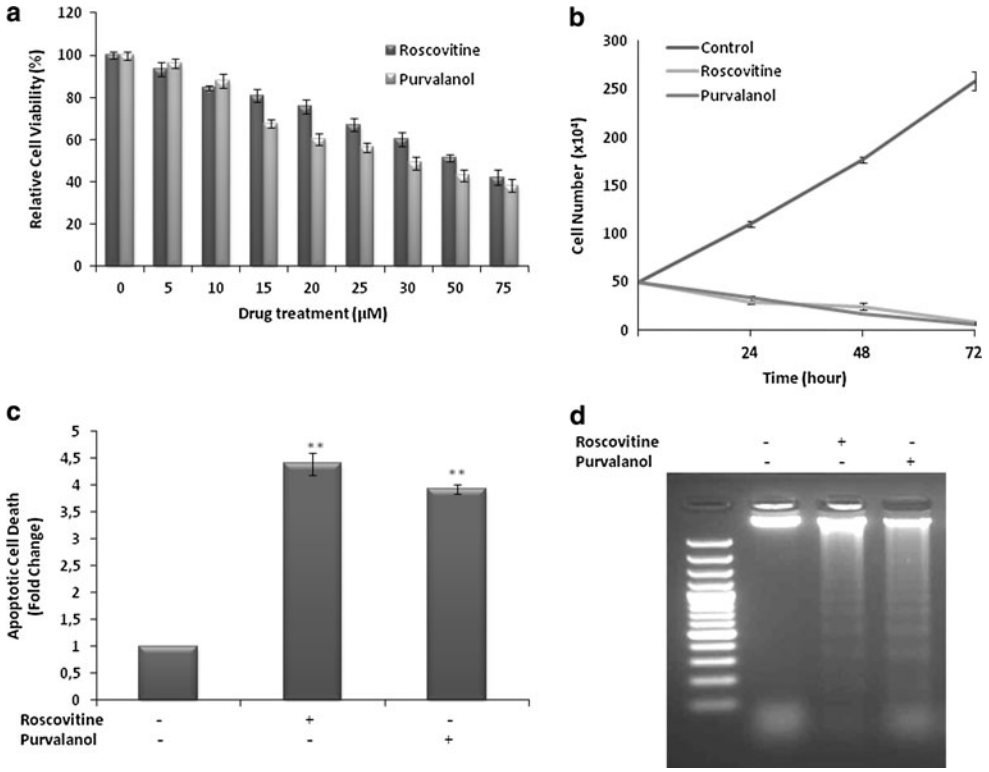

Fig. 1 Cytotoxic effect of CDK inhibitors (roscovitine and purvalanol) in HCT 116 colon carcinoma cells. **a** The effect of CDK inhibitors on cell viability was determined by the MTT cell viability assay after roscovitine or purvalanol (0–75 μM) treatment for 24 h. **b** HCT 116 cells were treated with 50 μM roscovitine or 30 μM purvalanol for 72 h and cells were stained with trypan blue at different time points; viable cells were counted under a light microscope. The data shown represent the mean ± SD from two experiments with three replicates. **c** Apoptotic cell death was determined using the Cell Death Detection ELISA^{PLUS} assay following exposure of HCT 116 cells to roscovitine (50 μM) or purvalanol (30 μM). Columns represent the mean ± SD from two independent trials with at least two replicates. Statistical differences were analyzed using an unpaired *t* test; $^*P < 0.05$. **d** HCT 116 cells were treated with roscovitine (50 μM) or purvalanol (30 μM) for 24 h. DNA fragments were extracted and analyzed on 2 % agarose gel

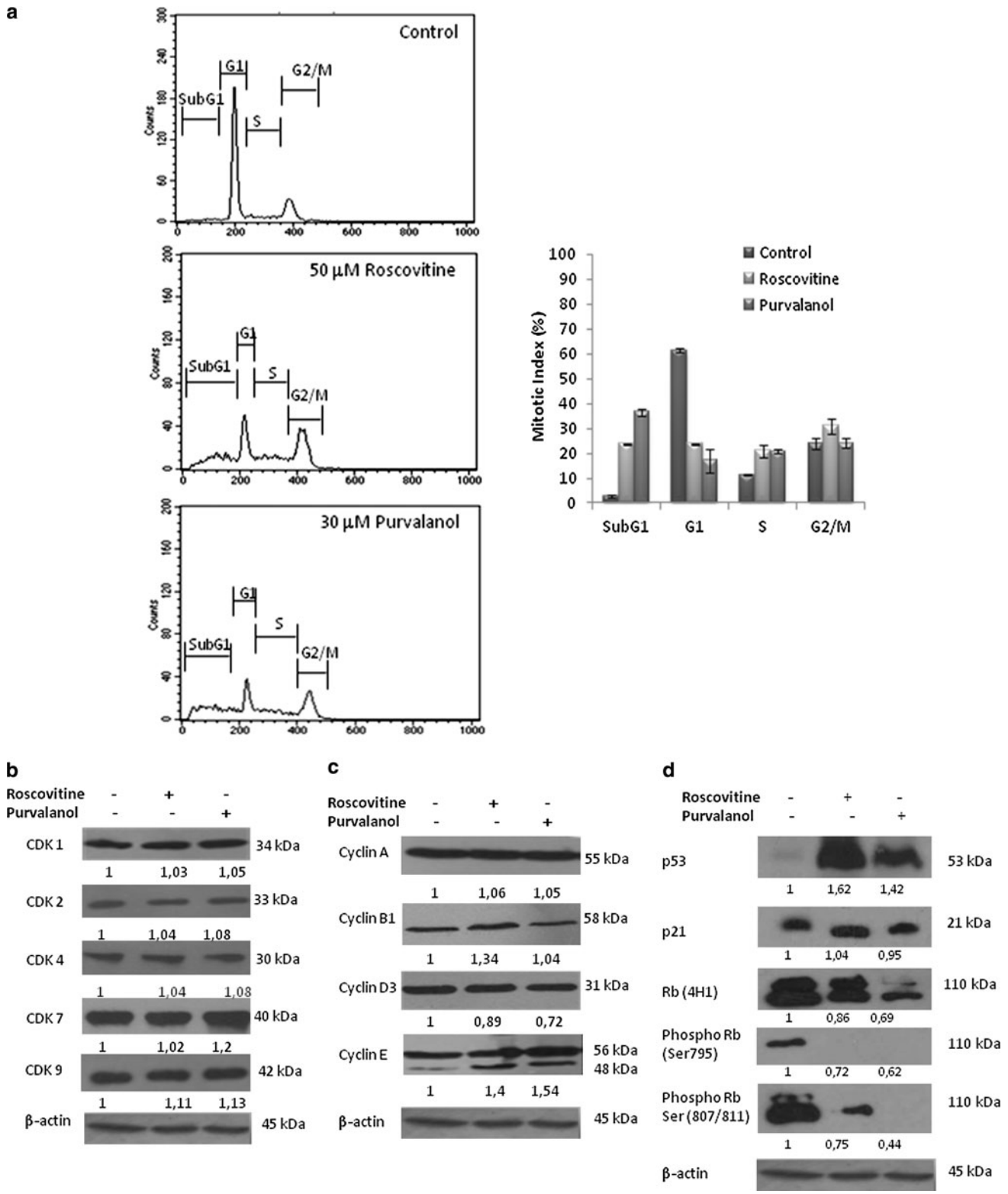

Fig. 2 Effects of roscovitine or purvalanol on cell cycle progression. **a** HCT 116 cells were treated with 50 µM roscovitine or 30 µM purvalanol for 24 h, and then cells were harvested, fixed with ethanol, and stained with propidium iodide. The cellular DNA contents were detected by flow cytometric analysis to determine the cell cycle distribution. Results shown are representative of three independent experiments. The effect of roscovitine or purvalanol treatment on gene expression profiles (**b** CDK; **c** cyclin; **d** p53, p21, and retinoblastoma (Rb)) was shown by immunoblotting. β-actin was used as a loading control

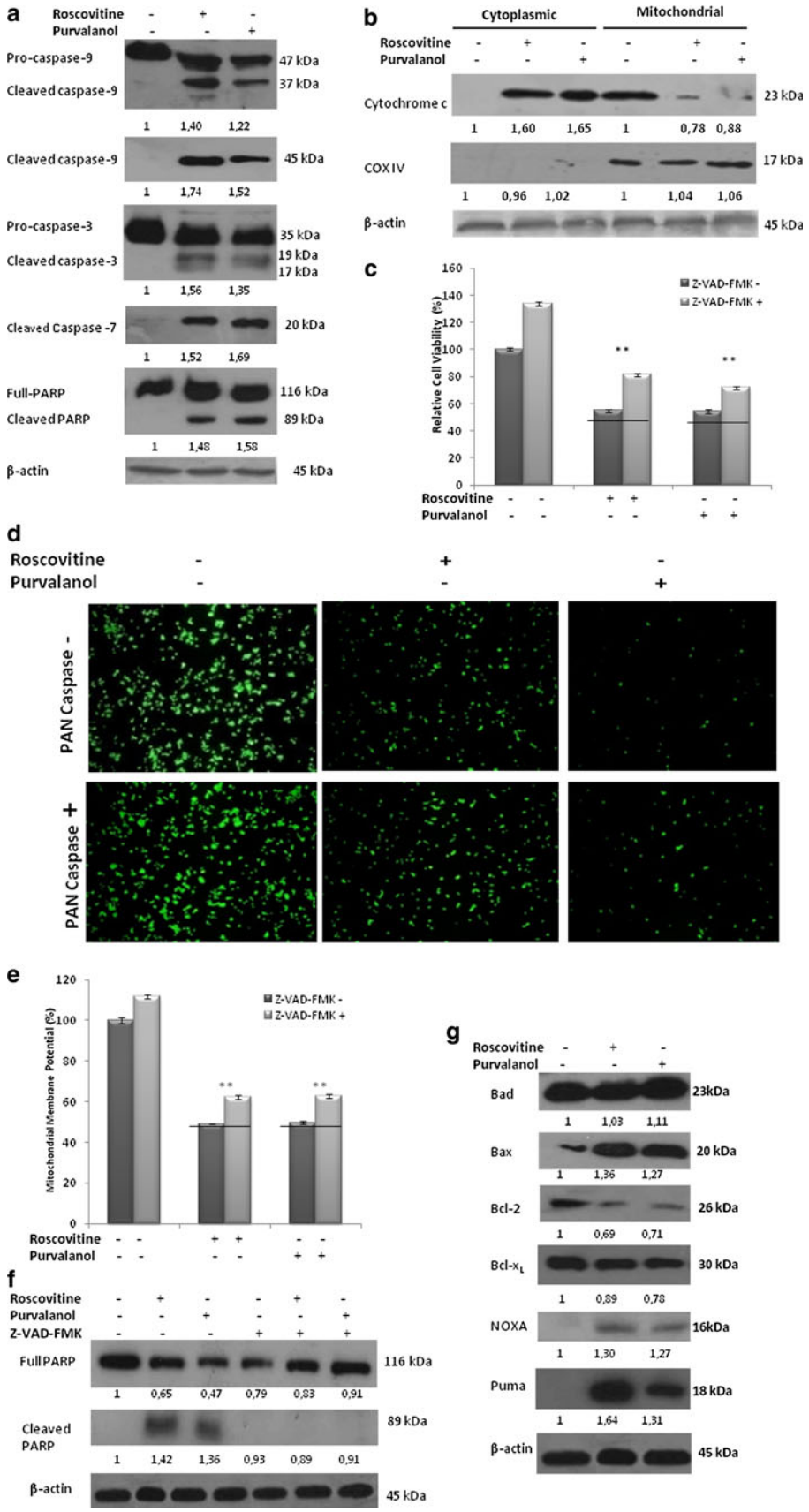
a
Roscovitine
Purvalanol
Pro-caspase-9
47 kDa
Cleaved caspase-9
37 kDa
1 1,40 1,22
Cleaved caspase-9
45 kDa
1 1,74 1,52
Pro-caspase-3
35 kDa
Cleaved caspase-3
19 kDa
17 kDa
1 1,56 1,35
Cleaved Caspase -7
20 kDa
1 1,52 1,69
Full-PARP
116 kDa
Cleaved PARP
89 kDa
1 1,48 1,58
β-actin
45 kDa
b
Cytoplasmic
Mitochondrial
Roscovitine
Purvalanol
Cytochrome c
23 kDa
1 1,60 1,65 1 0,78 0,88
COX IV
17 kDa
1 0,96 1,02 1 1,04 1,06
β-actin
45 kDa
c
Z-VAD-FMK -
Z-VAD-FMK +
Relative Cell Viability (%)
Roscovitine
Purvalanol
d
Roscovitine
Purvalanol
PAN Caspase -
PAN Caspase +
e
Z-VAD-FMK -
Z-VAD-FMK +
Mitochondrial Membrane Potential (%)
Roscovitine
Purvalanol
f
Roscovitine
Purvalanol
Z-VAD-FMK
Full PARP
116 kDa
1 0,65 0,47 0,79 0,83 0,91
Cleaved PARP
89 kDa
1 1,42 1,36 0,93 0,89 0,91
β-actin
45 kDa
g
Roscovitine
Purvalanol
Bad
23kDa
1 1,03 1,11
Bax
20 kDa
1 1,36 1,27
Bcl-2
26 kDa
1 0,69 0,71
Bcl-xL
30 kDa
1 0,89 0,78
NOXA
16kDa
1 1,30 1,27
Puma
18 kDa
1 1,64 1,31
β-actin
45 kDa

◀ **Fig. 3** CDK inhibitors induce apoptosis by activating caspases and modifying Bcl-2 family protein expression. **a** PARP cleavage and caspase-3, -7, and -9 activation in roscovitine (50 μM) or purvalanol (30 μM) treated HCT 116 cells were determined by immunoblotting. **b** The cytochrome *c* release induced by CDK inhibitors was determined by immunoblotting. Cytoplasmic and mitochondrial proteins were extracted using a mitochondrial fractionation kit and separated in a 12 % SDS-PAGE gel. COX IV was used as a loading control for the mitochondrial fractions. **c** Following a 2 h pretreatment of cells with general caspase inhibitor (10 μM Z-VAD-FMK), HCT 116 cells were treated with each CDK inhibitor for 24 h. Increases in cell viability following Z-VAD-FMK cotreatment were determined by the MTT cell viability assay. Statistical differences were analyzed using an unpaired *t* test; $*P < 0.05$, $**P < 0.001$. **d** Disruption of MMP was visualized by fluorescence microscopy (×200). **e** MMP loss was measured after $DiOC_6$ staining using a fluorometer (excitation = 485 nm, emission = 538 nm). Fluorometer results were obtained from two different culture conditions with at least four replicates. Statistical differences were analyzed using an unpaired *t* test; $*P < 0.05$, $**P < 0.001$. Columns represent the mean ± SD of five replicates from two different culture conditions. **f** Cleavage of PARP was assessed by immunoblotting. Thirty micrograms of total protein was loaded into each well. β-actin was used as a loading control. **g** The effect of roscovitine (50 μM) or purvalanol (30 μM) on Bcl-2 family protein expression in HCT 116 cells was determined by immunoblotting. Following CDK inhibitor treatments, total proteins were isolated and separated in a 12 % SDS gel, blotted on PVDF membranes, and incubated with antibodies to Bad, Bax, Bcl-2, Bcl-x_L, Noxa, and Puma. β-actin was used as a loading control

used to assess differences between control and treatment groups. Differences were regarded as statistically significant at values of $P < 0.05$.

Results

CDK inhibitors induce apoptosis by inhibiting cell proliferation potential

To determine the cytotoxic effect of each CDK inhibitor on HCT 116 colon carcinoma cells, we performed the MTT cell viability assay after treatment of cells with various concentrations (0–75 μM) of roscovitine or purvalanol for 24 h. According to the assay results, 50 μM roscovitine and 30 μM purvalanol decreased HCT 116 cell viability by 50 % (Fig. 1a).

We determined the effect of CDK inhibitors on cell proliferation using trypan blue staining. Exponentially growing HCT 116 cells were treated with roscovitine (50 μM) or purvalanol (30 μM) for 72 h, and viable cell counts were obtained every 24 h. While control cells were growing exponentially at every timepoint, treatment with CDK inhibitors prevented cell proliferation throughout the 72 h period (Fig. 1b).

The induction of apoptosis by CDK inhibitors was determined by a cell death ELISA assay. As shown in Fig. 1c, apoptosis was 4- and 3.5-fold higher in cells treated with 50 μM roscovitine or 30 μM purvalanol, respectively, than in untreated control cells ($P < 0.05$ and $P < 0.001$). Consistent with this observation, both CDK inhibitors induced DNA fragmentation in HCT 116 cells (Fig. 1d).

CDK inhibitors modulate cyclin expression profiles but not CDK expression profiles

To evaluate the effect of CDK inhibitors on cell cycle regulation in HCT 116 cells, we performed cell cycle analysis by flow cytometry. Each CDK inhibitor significantly induced cell cycle arrest at the G1/S phase transition. The subG1 population was 23.4 and 35.6 % larger in samples treated with roscovitine (50 μM) or purvalanol (30 μM), respectively, than in untreated control samples (Fig. 2a).

To further evaluate the effect of CDK inhibitors on cell cycle regulation in HCT 116 cells, we also determined the expression levels of several CDKs and cyclin molecules (Fig. 2b, c). The expression profiles of CDK 1, 2, 4, 7, and 9 were unchanged in roscovitine- and purvalanol-treated cells compared with control samples (Fig. 2b). However, both CDK inhibitors upregulated cyclin E (48 kDa), and purvalanol treatment triggered cyclin B1 downregulation in HCT 116 cells (Fig. 2c). Figure 2d shows that both CDK inhibitors upregulated p53 without any significant change in the expression of the p21 gene. Moreover, roscovitine and purvalanol treatment downregulated expression of the Rb gene and also suppressed the phosphorylation of Rb at Ser795 and Ser807/Ser811 (Fig. 2d).

Roscovitine and purvalanol activate the mitochondrial apoptotic pathway

To investigate the potential role of CDK inhibitors in caspase-dependent apoptosis, we examined caspase-3, -7, and -9 activation and PARP cleavage by immunoblotting following treatment of HCT 116 cells with CDK inhibitors (Fig. 3a). Roscovitine and purvalanol induced activation of caspase-3, -7, and -9. Exposure of cells to roscovitine or purvalanol for 24 h triggered PARP cleavage in a dose-dependent manner. Because mitochondria play a critical role in regulation of the apoptotic machinery, we measured MMP by cytochrome *c* release and $DiOC_6$ staining (Fig. 3b–f). Whereas cytochrome *c* was not detected in the cytoplasm of control cells, exposure of cells to roscovitine or purvalanol for 24 h induced release of cytochrome *c* from the mitochondria to the cytosol. This result was confirmed by the diminished amount of mitochondrial cytochrome *c* observed in HCT 116 cells following drug treatment (Fig. 3b). Moreover, cells cotreated with general caspase inhibitor (Z-VAD-FMK) and CDK inhibitors had greater

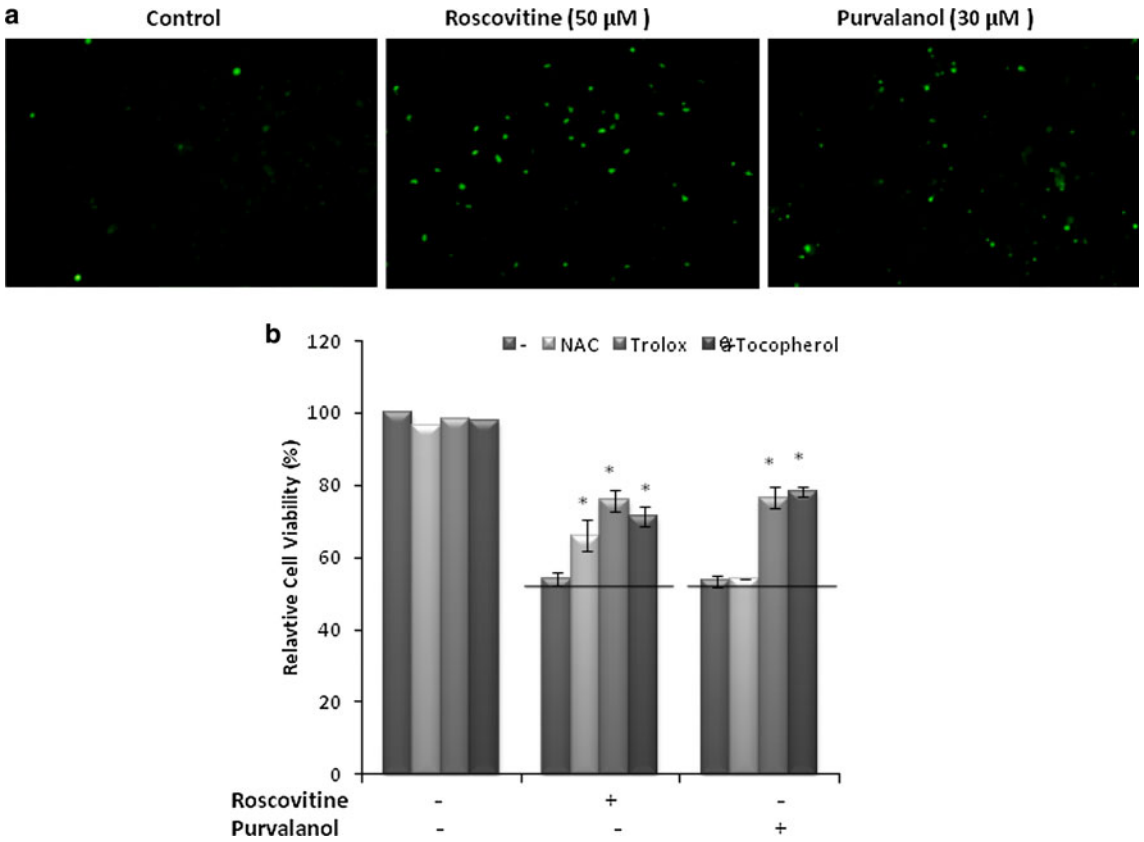

Fig. 4 CDK inhibitors induce ROS generation. **a** HCT 116 cells were seeded into a 96-well plate (1×10^4 cells/well) and treated with roscovitine (50 μM) or purvalanol (30 μM) for 24 h. Following DCFH-DA (1 μg/ml) staining for 30 min, ROS generation was visualized by fluorescence microscopy (×200 magnification). **b** HCT 116 cells were cotreated with CDK inhibitors and various antioxidants (5 μM NAC, 50 μM Trolox, 25 μM α-tocopherol). The MTT assay was performed to determine cell viability. Columns represent the mean ± SD from at least two experiments with four replicates. Statistical differences were analyzed using an unpaired *t* test; $^*P < 0.05$

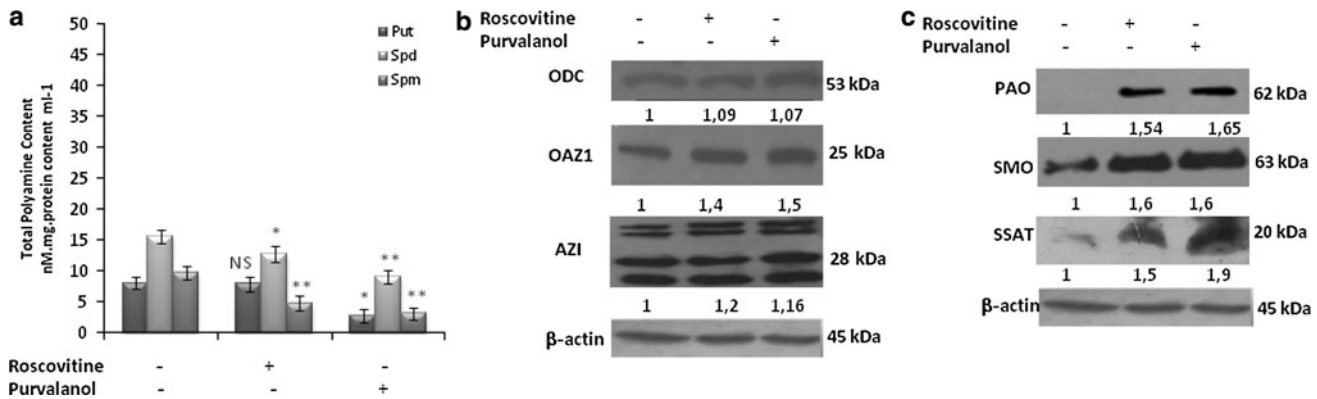

Fig. 5 The role of PA metabolism in CDK inhibitor-induced apoptotic cell death in HCT 116 cells. **a** The effect of roscovitine or purvalanol on intracellular PA levels was analyzed by HPLC; **b** gene expression profiles of PA biosynthetic and transport enzymes: ODC, OAZ1, and AZI; **c** expression profiles of PA catabolic enzymes (PAO, SSAT, SMO) in HCT 116 cells were determined by immunoblotting following 24 h treatments with roscovitine (50 μM) and purvalanol (30 μM). Statistical differences were analyzed using an unpaired *t* test; $^*P < 0.05$, $^{**}P < 0.001$; NS, not significant

viability than cells treated with CDK inhibitors alone (presence of Z-VAD-FMK: $P < 0.001$ vs. roscovitine, $P < 0.001$ vs. purvalanol) (Fig. 3c). Fluorescence microscopy and fluorometry (Fig. 3d, e) showed that exposure of cells to roscovitine (50 μM) or purvalanol (30 μM) for 24 h decreased MMP by 50 % ($P < 0.001$), and Z-VAD-FMK

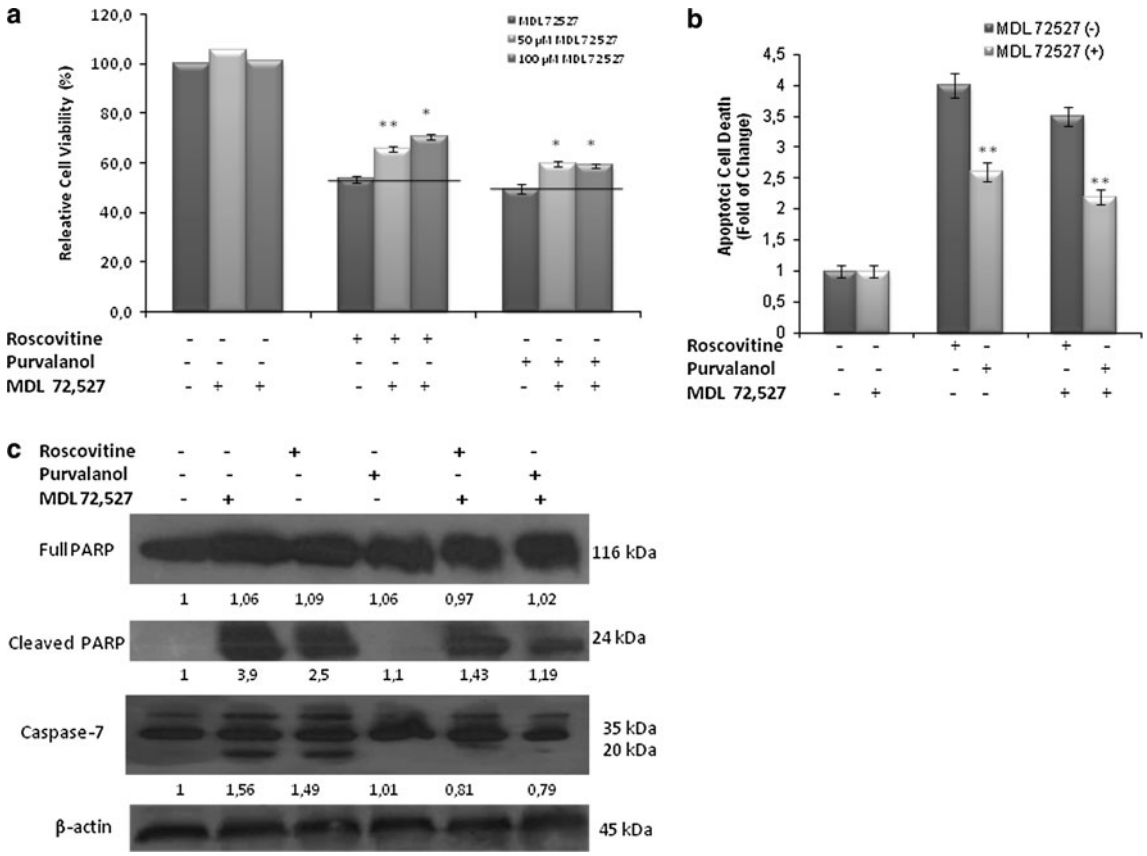

Fig. 6 Dose-dependent reversible effect of a PAO inhibitor (MDL-72,527) on roscovitine- or purvalanol-induced cell death. **a** MTT cell viability assay; **b** cell death ELISA; **c** immunoblotting was performed to examine the reversible effect of MDL-72,527 on roscovitine- or purvalanol-induced PARP cleavage and caspase-7 activation in HCT 116 cells. Columns represent the mean ± SD of at least two experiments with four replicates. Statistical differences were analyzed using an unpaired *t* test; $*P < 0.05$, $**P < 0.001$

cotreatment reduced the CDK inhibitor-induced MMP loss. In addition, Z-VAD-FMK cotreatment prevented CDK inhibitor-induced PARP cleavage (Fig. 3f).

To analyze the role of Bcl-2 family members in mitochondria-mediated apoptosis induced by treatment with CDK inhibitors, the expression of anti- and pro-apoptotic proteins was studied in HCT 116 cells by western blotting. Although both roscovitine and purvalanol downregulated Bcl-2 and Bcl-x_L, they had no significant effect on Bad expression. However, each CDK inhibitor upregulated Bax, Noxa, and Puma expression levels (Fig. 3g). Therefore, we conclude that both CDK inhibitors induced mitochondria-mediated apoptosis by activating caspases and modulating Bcl-2 family members.

CDK inhibitors induce generation of ROS

ROS generation is a critical factor in mitochondria-mediated apoptosis. For this reason, we determined ROS generation following drug treatment by DCFH-DA staining (Fig. 4a). The results indicated that roscovitine and purvalanol triggered generation of ROS in HCT 116 cells. We evaluated the effect of antioxidant molecules such as Trolox, α-tocopherol, and *N*-acetylcysteine (NAC) by determining the viability of cells cotreated with an antioxidant and a CDK inhibitor (50 μM roscovitine or 30 μM purvalanol). As shown in Fig. 4b, the loss of cell viability was greater in cells treated with roscovitine alone than in cells treated with the CDK inhibitor and an antioxidant ($P < 0.05$, $P < 0.001$, and $P < 0.05$ for Trolox, α-tocopherol, and NAC, respectively). Trolox and α-tocopherol but not the superoxide scavenger NAC reduced purvalanol-induced cytotoxicity ($P < 0.001$, $P < 0.05$, and $P = 0.229$, respectively) (Fig. 4b).

CDK inhibitors modulate PA metabolism

To examine the potential role of PAs in CDK inhibitor-induced apoptosis, we first determined the cellular PA content by HPLC (Fig. 5a). Exposure of cells to CDK inhibitors depleted putrescine ($P < 0.05$ for each inhibitor vs. control), spermidine, and spermine levels ($P < 0.001$ for each inhibitor vs. control).

To investigate the mechanism of PA depletion upon treatment with CDK inhibitors, we also determined the

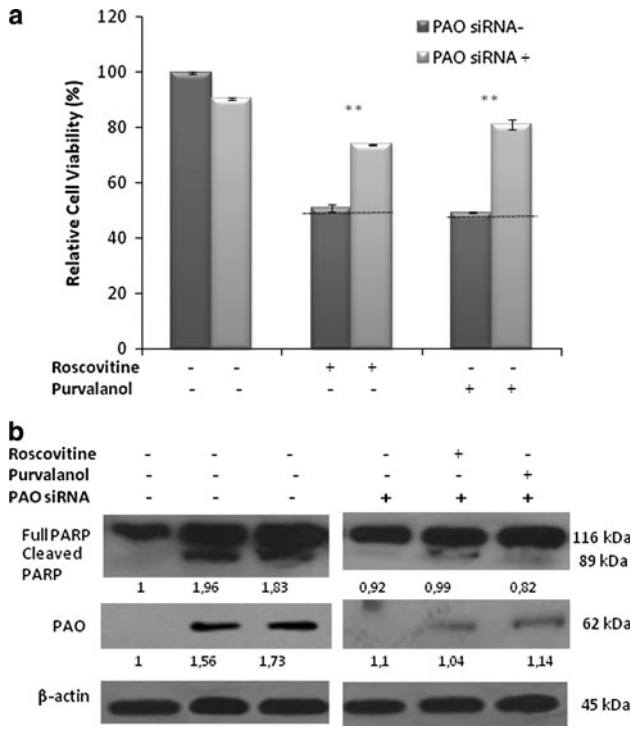

Fig. 7 Determination of CDK inhibitor-induced apoptosis in HCT 116 cells with transiently silenced PAO. Following transfection of HCT 116 cells with PAO siRNA and incubation for 48 h, roscovitine (50 μM) or purvalanol (30 μM) treatment was performed for 24 h. **a** The increase in cell viability because of PAO silencing was determined by the MTT cell viability assay. *Columns* represent the mean ± SD of two independent experiments with at least four replicates (*$P < 0.05$). **b** Prevention of CDK inhibitor-induced apoptotic cell death because of PAO silencing was determined by assessing PARP cleavage, and PAO silencing was confirmed by immunoblotting. Thirty micrograms of total protein was loaded into each well. β-actin was used as a loading control

expression profile of the biosynthetic enzyme ODC, and AZI and OAZ1, which regulate ODC activity (Fig. 5b). Although each CDK inhibitor upregulated AZI expression, no significant effect was observed for ODC or OAZ1 (Fig. 5b).

Interestingly, the PA catabolic enzymes PAO, SSAT, and SMO were found to be upregulated following exposure of cells to purvalanol or roscovitine for 24 h (Fig. 5c). Thus, we conclude that a major step in PA regulation in CDK inhibitor-induced apoptotic cell death is activation of catabolic enzymes. This finding was confirmed by the presence of highly elevated ROS levels suggesting accumulation of the byproducts of PA catabolism.

Inhibition of the PA catabolic pathway prevents CDK inhibitor-induced apoptosis

To investigate the potential role of the PA catabolic pathway in drug-induced apoptosis, we inhibited SMO and PAO using a specific inhibitor of these enzymes, MDL-72,527, and transiently silenced PAO gene expression by specific siRNA transfection. The loss of cell viability was greater in cells treated with a CDK inhibitor alone than in cells cotreated with purvalanol or roscovitine and MDL-72,527 ($P < 0.001$ and $P < 0.05$, respectively) (Fig. 6a). Moreover, cotreatment with MDL-72,527 (50 μM) reduced CDK inhibitor-induced apoptotic cell death (Fig. 6b). These results were confirmed by the decreased amounts of cleaved PARP (89 kDa) and caspase-7 observed in cells cotreated with MDL-72,527 (Fig. 6c). Additionally, transient silencing of PAO gene expression by PAO siRNA significantly reduced both the cell viability loss (Fig. 7a) and the PAO upregulation (Fig. 7b) induced by treatment with CDK inhibitors. Moreover, CDK inhibitor-induced apoptotic cell death because of PAO expression was reduced by PAO siRNA (Fig. 7b).

Discussion

Aberrant cell cycle regulation is one of the remarkable characteristics of cancer. New CDK inhibitors such as roscovitine and purvalanol are important potential therapeutic agents because of their apoptotic potential against malignant cells [25]. Recent studies have shown that roscovitine might induce apoptosis in MCF-7, HeLa, SW480, SW1116, and SW837 cells by binding specific CDK targets and preventing complex formation with cyclins [9, 25–28]. Roscovitine was shown to inhibit CDK1, CDK2, and CDK5, and inhibition of these molecules led to induction of cell cycle arrest at the G1/S or G2/M phase transition in MCF-7 [29], lung cancer [8], HeLa [30], and HCT 116 colon cancer cells [10]. Purvalanol might act as an antiproliferative agent with apoptotic potential by inducing cell cycle arrest in Chinese hamster lung fibroblast cell lines and MCF-7 cells [9, 31]. Similarly, in this study we found that roscovitine or purvalanol treatment caused a significant decrease in cell proliferation and induced apoptosis in HCT 116 colon carcinoma cells (Fig. 1c, d). We determined that cell cycle arrest at the G1/S phase transition was induced by roscovitine (50 μM) or purvalanol (30 μM) treatment. Although both of these treatments decreased cell viability by 50 % compared with the control, the increase in the subG1 population was greater in purvalanol-treated HCT 116 cells than in roscovitine-treated cells (Fig. 2a). As CDK inhibitors, roscovitine and purvalanol did not significantly alter the expression profiles of CDKs but did induce cyclin E upregulation. Purvalanol upregulated cyclin B1 expression but roscovitine did not exert the same effect in HCT 116 cells.

CDK inhibitors and other well-known chemotherapeutic agents activate the mitochondria-mediated apoptotic

pathway [32]. A number of reports have shown that roscovitine exerts its apoptotic function by activating caspases and mitochondria-mediated apoptosis in breast [29], leukemia [33], lung [8], and colon cancer cells [10]. Similarly, we found that exposure of HCT 116 cells to roscovitine or purvalanol for 24 h induced modulation of MMP, as indicated by cytochrome *c* release (Fig. 3b). We also found that roscovitine or purvalanol treatment resulted in caspase-3, -7, and -9 activation and PARP cleavage, which are key signatures of apoptotic induction (Fig. 3a). In addition, the presence of a caspase inhibitor protected HCT 116 cells against CDK inhibitor-induced cytotoxicity (Fig. 3c). Moreover, addition of the caspase inhibitor (Z-VAD-FMK) with roscovitine or purvalanol reduced MMP loss and PARP cleavage (Fig. 3d–f). Therefore, we conclude that the apoptotic induction was reversible following treatment with CDK inhibitors for 24 h. We showed that roscovitine or purvalanol treatment modulated expression of the Bcl-2 family members in HCT 116 cells (Fig. 3g). It was previously reported that both caspase activation and ROS generation are observed in drug-induced apoptotic induction [34]. In this study, using DCFH-DA staining, we found that the CDK inhibitors induced ROS generation. The presence of ROS-scavenging agents (except the superoxide-scavenging agent NAC) reduced the cytotoxic effects of CDK inhibitors in HCT 116 cells (Fig. 4a, b).

In the second part of this study, we investigated the potential role of PAs in CDK inhibitor-induced apoptosis in HCT 116 colon carcinoma cells. It is well documented that intracellular PAs are essential for various cellular processes such as growth, differentiation, and proliferation in all organisms [12, 35]. Elevated PA levels may be a potential biomarker for malignant disease [36]. Therefore, several therapeutic strategies that target PA metabolism are being investigated [37]. Despite the availability of PA analogues and our knowledge about the interactions of classical chemotherapeutic agents with PA metabolism [10, 38, 39], the functional role of PAs in cell death has not yet been clarified. We determined that HCT 116 cells exposed to roscovitine or purvalanol had lower PA levels than untreated control cells (Fig. 5a–c). Also, these CDK inhibitors activated PA catabolic enzymes but had no significant effect on the biosynthetic enzyme ODC. The drugs upregulated AZI expression but did not affect OAZ1 expression. We conclude that while the CDK inhibitors induced cell cycle arrest, they also decreased the intracellular PA pool by increasing catabolic activity without affecting intracellular PA biosynthesis signaling. Therefore, these drugs act as PA analogues, which successfully upregulate SSAT expression in cancer cells [40, 41]. SSAT upregulation following drug treatment has been demonstrated by DNA microarray screening of cells [21]. Like SSAT, PAO is one of the key enzymes of the PA catabolic pathway; this enzyme causes generation of H_2O_2 [18] and was upregulated by roscovitine treatment in HCT 116 cells. To clarify the potential role of PAO in CDK inhibitor-induced apoptosis, we cotreated cells with MDL-72,527 (a PAO/SMO inhibitor) and roscovitine or purvalanol for 24 h. Recent studies have shown that MDL-72,527 prevents apoptosis by blocking the acetylation of PAs and decreasing H_2O_2 production [42]. MDL-72,527 might block the agonistic toxic effect of SSAT in Chinese Hamster Ovary (CHO) and non-small cell lung cancer cells [43, 44]. However, exposure of B cells to MDL-72,527 induced apoptosis by increasing lysosomotropic effects [45]. Previous studies have indicated that the response to MDL-72,527 cotreatment is cell type specific; in our experimental system MDL-72,527 (50 μM) had no cytotoxic effect on HCT 116 colon carcinoma cells (Fig. 6a). We found that inhibition of PAO by MDL-72,527 (Fig. 6b, c) and transient silencing of PAO by PAO siRNA abrogated CDK inhibitor-induced apoptotic cell death (Fig. 7a). Therefore, we conclude that CDK inhibitors as strong apoptotic inducers may decrease PA levels by activating PA catabolism. However, any defect of the PA catabolic pathway might be critical for the therapeutic efficacy of CDK inhibitors.

Acknowledgments The authors thank Tuğba Kızılboğa for technical assistance during the study. This study was supported by TUBITAK (The Scientific and Technical Research. Council of Turkey, Project number: 108T630) and Istanbul Kultur University Scientific Projects Support Center.

Conflict of interest The authors declare that they have no conflict of interest.

References

1. Duranton B, Holl V, Schneider Y et al (2002) Cytotoxic effects of the polyamine oxidase inactivator MDL 72527 to two human colon carcinoma cell lines SW480 and SW620. Cell Biol Toxicol 18:381–396
2. Benassi MS, Molendini L, Gamberi G et al (1999) Alteration of pRb/p16/cdk4 regulation in human osteosarcoma. Int J Cancer 84:489–493
3. King KL, Cidlowski JA (1995) Cell cycle and apoptosis: common pathways to life and death. J Cell Biochem 58:175–180
4. McClue SJ, Blake D, Clarke R et al (2002) In vitro and in vivo antitumor properties of the cyclin dependent kinase inhibitor CYC202 (R-roscovitine). Int J Cancer 102:463–468
5. Meijer L, Borgne A, Mulner O et al (1997) Biochemical and cellular effects of roscovitine, a potent and selective inhibitor of the cyclin-dependent kinases cdc2, cdk2 and cdk5. Eur J Biochem 243:527–536
6. Mohapatra S, Chu B, Zhao X, Djeu J, Cheng JQ, Pledger WJ (2009) Apoptosis of metastatic prostate cancer cells by a combination of cyclin-dependent kinase and AKT inhibitors. Int J Biochem Cell Biol 41:595–602
7. Wesierska-Gadek J, Gritsch D, Zulehner N, Komina O, Maurer M (2011) Roscovitine, a selective CDK inhibitor, reduces the basal and estrogen-induced phosphorylation of ER-α in human ER-positive breast cancer cells. J Cell Biochem 112:761–772

8. Zhang T, Jiang T, Zhang F et al (2010) Involvement of p21Waf1/Cip1 cleavage during roscovitine-induced apoptosis in non-small cell lung cancer cells. Oncol Rep 23:239–245
9. Raje N, Kumar S, Hideshima T et al (2005) Seliciclib (CYC202 or R-roscovitine), a small-molecule cyclin-dependent kinase inhibitor, mediates activity via down-regulation of Mcl-1 in multiple myeloma. Blood 106:1042–1047
10. Arisan ED, Coker A, Palavan-Unsal N (2012) Polyamine depletion enhances the roscovitine-induced apoptosis through the activation of mitochondria in HCT116 colon carcinoma cells. Amino Acids 42:655–665
11. Pegg AE, McCann PP (1982) Polyamine metabolism and function. Am J Physiol 243:C212–C221
12. Heby O, Persson L (1990) Molecular genetics of polyamine synthesis in eukaryotic cells. Trends Biochem Sci 15:153–158
13. Heby O, Andersson G, Gray JW (1978) Interference with S and G2 phase progression by polyamine synthesis inhibitors. Exp Cell Res 111:461–464
14. Andersson G, Heby O (1977) Kinetics of cell proliferation and polyamine synthesis during Ehrlich ascites tumor growth. Cancer Res 37:4361–4366
15. Morgan DML (1998) Polyamines: an introduction. In: Morgan DML (ed) Polyamine protocols. Humana Press, Clifton, pp 3–30
16. Hsu PC, Hung HC, Liao YF, Liu CC, Tsay GJ, Liu GY (2008) Ornithine decarboxylase attenuates leukemic chemotherapy drugs-induced cell apoptosis and arrest in human promyelocytic HL-60 cells. Leuk Res 32:1530–1540
17. Hu HY, Liu XX, Jiang CY et al (2005) Ornithine decarboxylase gene is overexpressed in colorectal carcinoma. World J Gastroenterol 11:2244–2248
18. Parchment RE, Pierce GB (1989) Polyamine oxidation, programmed cell death, and regulation of melanoma in the murine embryonic limb. Cancer Res 49:6680–6686
19. Casero RA Jr, Pegg AE (1993) Spermidine/spermine N^1-acetyltransferase—the turning point in polyamine metabolism. Faseb J 7:653–661
20. Wu T, Yankovskaya V, McIntire WS (2003) Cloning, sequencing, and heterologous expression of the murine peroxisomal flavoprotein, N^1-acetylated polyamine oxidase. J Biol Chem 278:20514–20525
21. Allen WL, McLean EG, Boyer J et al (2007) The role of spermidine/spermine N^1-acetyltransferase in determining response to chemotherapeutic agents in colorectal cancer cells. Mol Cancer Ther 6:128–137
22. Coker A, Arisan ED, Palavan-Unsal N (2012) Silencing of the polyamine catabolic key enzyme SSAT prevents CDK inhibitor-induced apoptosis in CaCo-2 colon cancer cells. Mol Med Rep 5:1037–1042
23. Garrofé-Ochoa X, Cosialls AM, Ribas J, Gil J, Boix J (2011) Transcriptional modulation of apoptosis regulators by roscovitine and related compounds. Apoptosis 16(7):660–670
24. Haan C, Behrmann I (2007) A cost effective non-commercial ECL-solution for Western blot detections yielding strong signals and low background. J Immunol Methods 318:11–19
25. Senderowicz AM (2003) Novel direct and indirect cyclin-dependent kinase modulators for the prevention and treatment of human neoplasms. Cancer Chemother Pharmacol 52:S61–S73
26. Maurer M, Komina O, Wesierska-Gadek J (2009) Roscovitine differentially affects asynchronously growing and synchronized human MCF-7 breast cancer cells. Ann N Y Acad Sci 1171:250–256
27. Villerbu N, Gaben AM, Redeuilh G, Mester J (2002) Cellular effects of purvalanol A: a specific inhibitor of cyclin-dependent kinase activities. Int J Cancer 97:761–769
28. Abaza MS, Bahman AM, Al-Attiyah RJ (2008) Roscovitine synergizes with conventional chemo-therapeutic drugs to induce efficient apoptosis of human colorectal cancer cells. World J Gastroenterol 14:5162–5175
29. Wesierska-Gadek J, Gueorguieva M, Wojciechowski J, Horky M (2004) Cell cycle arrest induced in human breast cancer cells by cyclin-dependent kinase inhibitors: a comparison of the effects exerted by roscovitine and olomoucine. Pol J Pharmacol 56:635–641
30. Wesierska-Gadek J, Wandl S, Kramer MP, Pickem C, Krystof V, Hajek SB (2008) Roscovitine up-regulates p53 protein and induces apoptosis in human HeLaS(3) cervix carcinoma cells. J Cell Biochem 105:1161–1171
31. Knockaert M, Lenormand P, Gray N, Schultz P, Pouyssegur J, Meijer L (2002) p42/p44 MAPKs are intracellular targets of the CDK inhibitor purvalanol. Oncogene 21:6413–6424
32. Herr I, Debatin KM (2001) Cellular stress response and apoptosis in cancer therapy. Blood 98:2603–2614
33. Hahntow IN, Schneller F, Oelsner M et al (2004) Cyclin-dependent kinase inhibitor roscovitine induces apoptosis in chronic lymphocytic leukemia cells. Leukemia 18:747–755
34. Rosato RR, Almenara JA, Maggio SC et al (2005) Potentiation of the lethality of the histone deacetylase inhibitor LAQ824 by the cyclin-dependent kinase inhibitor roscovitine in human leukemia cells. Mol Cancer Ther 4:1772–1785
35. Hamana K, Matsuzaki S (1992) Polyamines as a chemotaxonomic marker in bacterial systematics. Crit Rev Microbiol 18:261–283
36. McGarrity TJ, Peiffer LP, Bartholomew MJ, Pegg AE (1990) Colonic polyamine content and ornithine decarboxylase activity as markers for adenomas. Cancer 66:1539–1543
37. Pegg AE (1988) Polyamine metabolism and its importance in neoplastic growth and a target for chemotherapy. Cancer Res 48:759–774
38. Devens BH, Weeks RS, Burns MR, Carlson CL, Brawer MK (2000) Polyamine depletion therapy in prostate cancer. Prostate Cancer Prostatic Dis 3:275–279
39. Kramer DL, Chang BD, Chen Y et al (2001) Polyamine depletion in human melanoma cells leads to G1 arrest associated with induction of p21WAF1/CIP1/SDI1, changes in the expression of p21-regulated genes, and a senescence-like phenotype. Cancer Res 61:7754–7762
40. Casero RA Jr, Woster PM (2001) Terminally alkylated polyamine analogues as chemotherapeutic agents. J Med Chem 44: 1–26
41. Casero RA Jr, Celano P, Ervin SJ, Wiest L, Pegg AE (1990) High specific induction of spermidine/spermine N^1-acetyltransferase in a human large cell lung carcinoma. Biochem J 270:615–620
42. Bolkenius FN, Bey P, Seiler N (1985) Specific inhibition of polyamine oxidase in vivo is a method for the elucidation of its physiological role. Biochim Biophys Acta 838:69–76
43. Hu RH, Pegg AE (1997) Rapid induction of apoptosis by deregulated uptake of polyamine analogues. Biochem J 328: 307–316
44. Ha HC, Woster PM, Yager JD, Casero RA Jr (1997) The role of polyamine catabolism in polyamine analogue-induced programmed cell death. Proc Natl Acad Sci USA 94:11557–11562
45. Dai H, Kramer DL, Yang C, Murti KG, Porter CW, Cleveland JL (1999) The polyamine oxidase inhibitor MDL-72,527 selectively induces apoptosis of transformed hematopoietic cells through lysosomotropic effects. Cancer Res 59:4944–4954